The impact of maturation delay of mosquitoes on the transmission of West Nile virus ☆

Guihong Fan [a], Junli Liu [b], P. van den Driessche [c], Jianhong Wu [a], Huaiping Zhu [a,*]

[a] Centre for Disease Modeling, Laboratory of Mathematical Parallel Systems, Laboratory for Industrial and Applied Mathematics, Department of Mathematics and Statistics, York University, Toronto, ON, Canada M3J 1P3
[b] School of Science, Xi'an Polytechnic University, Xi'an 710048, PR China
[c] Department of Mathematics and Statistics, University of Victoria, Victoria, BC, Canada V8W 3R4

A B S T R A C T

We formulate and analyze a delay differential equation model for the transmission of West Nile virus between vector mosquitoes and avian hosts that incorporates maturation delay for mosquitoes. The maturation time from eggs to adult mosquitoes is sensitive to weather conditions, in particular the temperature, and the model allows us to investigate the impact of this maturation time on transmission dynamics of the virus among mosquitoes and birds. Numerical results of the model show that a combination of the maturation time and the vertical transmission of the virus in mosquitoes has substantial influence on the abundance and number of infection peaks of the infectious mosquitoes.

© 2010 Elsevier Inc. All rights reserved.

1. Introduction

West Nile virus (WNv) is transmitted among mosquitoes, birds, humans, and other animals. Mosquitoes are the vector of the virus and birds are its natural reservoir, whereas humans, horses and probably other vertebrates are circumstantial hosts; that is, they can be infected by an infectious mosquito but they do not transmit the disease. Thus the virus is maintained in nature in a mosquito-bird-mosquito transmission cycle ([8,21]). When an infectious mosquito bites a susceptible bird, it can transmit the virus to the bird, and the bird may then develop sufficiently high viral titers in three to five days to infect mosquitoes. The virus can also be passed via vertical transmission from a mosquito to its offsprings ([1,15]) and this increases the survival probability of WNv in nature. It is reasonable to believe that this vertical transmission was the mechanism responsible for the persistence of epidemics in New York after the winter of 1999.

Much has been done in terms of modeling and analysis of transmission dynamics of WNv, see, for example Bowman et al. [6], Lewis et al. [25], Wan and Zhu [37] and Wonham et al. [38]. But none of these models have considered the effect of temperature on the transmission of the virus spread. Estimating the potential impact of climate change on WNv transmission is of great importance due to the concern that this virus may emerge or re-emerge in many parts of the world. Global warming may affect the future pattern of many arthropod-borne diseases, yet the relationship between temperature and the transmission mechanisms for many key vectors has been mostly ignored. The rate at which new individual mosquitoes develop from eggs is one of the key factors that determines the growth rate of the mosquitoes. This rate is critically dependent on the growth characteristics of immature stages, which is governed by temperature, where food is not limited [24]. The influence of temperature on these stages has been studied in a number of different species of mosquitoes, including *Anopheles quadrimaculatus Say* [20], *Aedes aegypti Linnaeus* [34].

In general, within the limits of a lower development threshold and an upper lethal temperature, the aquatic stages of mosquitoes develop faster as temperature increases ([7,18]). The shortening of aquatic life is important since it increases adult mosquito turnover, with consequences for increased vector biting rate and disease transmission [14]. There have been some modeling studies for other mosquito borne diseases incorporating the impact of temperature. For example, in the study of St. Louis encephalitis virus, Lord and Day [26] used a modified cosine function of time as a driving function for the vector mortality rate and the length of the latent

period, and in a recent paper Paaijmans et al. [30] studied the effect of temperature on mosquitoes in the context of malaria.

The life cycle of the mosquito consists of three successive aquatic juvenile phases (egg, larva and pupa) and one adult pupa [39]. It usually takes 1–2 weeks from the egg to the adult, which is large compared to the average life span (about 3 weeks) of an adult mosquito. The size of the mosquito population is strongly affected by temperature ([5,31]). The number of female mosquitoes changes accordingly due to seasonal variations. During the favorable periods when the size of the mosquito population increases, the risk of WNv infection among birds also increases, therefore the incidence for humans increases. So, it is important to consider the maturation time, the length of the larval phase from egg to adult mosquitoes, and its impact on the transmission of WNv.

In this paper, we first formulate (in Section 2) a model of delay differential equations to explore the temporal mosquito-bird cycle transmission of WNv. It consists of the interactions among susceptible and infectious individuals of the two species assuming that the transmission of the virus is only by the bites of mosquitoes and vertical transmission in the vector population. Section 3 classifies the equilibria and describes the global dynamics of the model system. In Section 4 we present some simulation results. We investigate the effects of maturation delay due to the temperature on the number of mosquitoes and on WNv spread among mosquitoes and birds. The analysis and simulations reveal that, with the combination of the maturation delay and vertical transmission of mosquitoes, the model can exhibit rich dynamics.

2. Model formulation and global dynamics of mosquitoes

Let $M_s(t)$ and $M_i(t)$ denote the number of susceptible and infectious female adult mosquitoes.

The total female mosquito population is $N_M(t) = M_s(t) + M_i(t)$. Though more than one species of birds are involved in the transmission of the virus, as in the models mentioned in the introduction and for simplicity, we consider the birds as one family, and let $B_s(t)$, $B_i(t)$, and $B_r(t)$ be the number of susceptible, infectious, and recovered birds, respectively. The total bird population is $N_B(t) = B_s(t) + B_i(t) + B_r(t)$.

Since the development of mosquitoes from eggs to adults is density dependent, a Ricker type function is taken for the birth rate into the adult mosquitoes. This function has been used for example in [11] and to model the vector population of Chagas disease [36]. Let the finite constant $\tau \geqslant 0$ be the maturation time of the mosquito, i.e., the average time needed for an egg to develop into an adult mosquito, and let $d_j \geqslant 0$ be the death rate of juvenile mosquitoes. Then the birth rate function of mosquitoes is taken as $r_m N_M(t-\tau)e^{-d_j\tau}e^{-\alpha N_M}$, where $r_m > 0$ is the maximum per capita daily mosquito egg production rate, and $\frac{1}{\alpha}$ (with $\alpha > 0$) is the size of the mosquito population at which egg laying is maximized when maturation delay is ignored. The term $r_m N_M(t-\tau)$ represents the mosquito eggs laid τ units ago and $e^{-d_j\tau}$ reflects the survival probability to become an adult mosquito over the maturation period. Even if mosquito eggs survive the maturation period, the current environment determines whether or not they can turn over to adult mosquitoes, hence the Ricker type birth rate function $e^{-\alpha N_M}$ has N_M at the current time. The parameter $d_m > 0$ is the natural death rate of adult female mosquitoes. Vertical transmission of the virus in the mosquito population is incorporated by a fraction $q \in [0, 1)$ of births from infectious mosquitoes going directly to the infectious mosquito class. The cross-infection between birds and mosquitoes is modeled using mass action incidence (see [19]) normalized by total bird population (see also [2]). Parameters β_m and β_b are the contact transmission rates between infectious birds to

susceptible mosquitoes and infectious mosquitoes to susceptible birds, respectively. The parameter $\mu > 0$ is the West Nile virus induced death rate of infectious birds, and the parameter $v > 0$ denotes the recovery rate of the infectious birds. In this annual model, it is reasonable to assume that the demographic dynamics for birds can be ignored, as the natural birth and death are balanced in the absence of virus. Though there is evidence shown (see [23,28]) that bird to bird transmission of the virus is possible, the contact transmission probability is low and hence is neglected in this study. The above assumptions lead to the following system

$$\begin{cases} \frac{dM_s(t)}{dt} = r_m M_s(t-\tau)e^{-d_j\tau}e^{-\alpha N_M(t)} - \frac{\beta_m M_s(t)B_i(t)}{N_B(t)} - d_m M_s(t) \\ \qquad + (1-q)r_m M_i(t-\tau)e^{-d_j\tau}e^{-\alpha N_M(t)}, \\ \frac{dM_i(t)}{dt} = q r_m M_i(t-\tau)e^{-d_j\tau}e^{-\alpha N_M(t)} + \frac{\beta_m M_s(t)B_i(t)}{N_B(t)} - d_m M_i(t), \\ \frac{dB_s(t)}{dt} = -\frac{\beta_b M_i(t)B_s(t)}{N_B(t)}, \\ \frac{dB_i(t)}{dt} = \frac{\beta_b M_i(t)B_s(t)}{N_B(t)} - (\mu+v)B_i(t), \\ \frac{dB_r(t)}{dt} = v B_i(t), \end{cases} \quad (2.1)$$

with initial data

$$M_s(\theta) = \phi_s(\theta) > 0, \quad M_i(\theta) = \phi_i(\theta) > 0,$$

$$B_s(0) = B_{s0} > 0, \quad B_i(0) = B_{i0} \geqslant 0, \quad B_r(0) = B_{r0} \geqslant 0, \quad (2.2)$$

where $\phi_s(\theta)$ and $\phi_i(\theta)$ are positive continuous functions of $\theta \in [-\tau, 0]$. Later we will show that for $t \geqslant 0$, $N_B(t) \neq 0$. This conclusion will guarantee the existence and uniqueness of solutions.

It follows from (2.1) that the total number of adult female mosquitoes satisfies the following equation:

$$\frac{dN_M(t)}{dt} = r_m N_M(t-\tau)e^{-d_j\tau}e^{-\alpha N_M(t)} - d_m N_M(t), \quad (2.3)$$

with initial data

$$N_M(\theta) = \phi_s(\theta) + \phi_i(\theta) > 0 \quad \text{for} \quad \theta \in [-\tau, 0]. \quad (2.4)$$

Letting

$$N_M^* = \frac{1}{\alpha}\ln(\frac{r_m}{d_m e^{d_j\tau}}), \quad (2.5)$$

it follows that $N_M = N_M^*$ is the unique positive equilibrium for the mosquito Eq. (2.3), and this exists if and only if $r_m e^{-d_j\tau} > d_m$. Defining $h = \frac{1}{2}\min\{\min_{\theta \in [-\tau,0]}\{\phi_s(\theta) + \phi_i(\theta)\}, N_M^*\}$ and $H = 1 + \max\{\max_{\theta \in [-\tau,0]}\{\phi_s(\theta) + \phi_i(\theta)\}, N_M^*\}$, the following theorem describes the global asymptotic behavior of (2.3) (see [4], Theorem 2.3).

Theorem 2.1. *For system (2.3) with initial data (2.4), the solution $N_M(t)$ is positive for any finite time $t \geqslant 0$.*

(i) *If $r_m e^{-d_j\tau} \leqslant d_m$, then the solution $N_M(t)$ is bounded and the trivial equilibrium $N_M = 0$ is globally asymptotically stable with respect to the positive initial data.*

(ii) *If $r_m e^{-d_j\tau} > d_m$, then $h < N_M(t) < H$ for any $t \geqslant 0$. Moreover there exists a positive equilibrium N_M^* that is globally asymptotically stable.*

Proof. We use the method of contradiction to prove that $N_M(t) > 0$ for any finite $t \geqslant 0$. Noting that $N_M(\theta) > 0$ for any $\theta \in [-\tau, 0]$, suppose that there exists a $\hat{t} > 0$ such that $N_M(\hat{t}) = 0$, $N_M(t) > 0$ for $t < \hat{t}$, and $\frac{dN_M(\hat{t})}{dt} \leqslant 0$. It follows from (2.3) that

$$\frac{dN_M(\hat{t})}{dt} = r_m N_M(\hat{t}-\tau)e^{-d_j\tau} > 0,$$

a contradiction. Hence $N_M(t) > 0$ for any finite $t \geqslant 0$.

We next prove that solutions are bounded in cases (i) and (ii).

Case (i) Assume that $r_m e^{-d_j\tau} \leqslant d_m$. Let $L = \max_{\theta\in[-\tau,\,0]}\{\phi_s(\theta) + \phi_i(\theta)\}$. Then $N_M(t) \leqslant L$. Otherwise there exists a $\bar{t} > 0$ such that $N_M(\bar{t}) = L$, $N_M(t) \leqslant L$ for any $t < \bar{t}$, and $\frac{dN_M(\bar{t})}{dt} \geqslant 0$. From (2.3),

$$\frac{dN_M(\bar{t})}{dt} = r_m N_M(\bar{t} - \tau)e^{-d_j\tau}e^{-\alpha L} - d_m L \leqslant L(r_m e^{-d_j\tau}e^{-\alpha L} - d_m)$$
$$< L(r_m e^{-d_j\tau} - d_m) \leqslant 0,$$

a contradiction. Hence $N_M(t) \leqslant L$ for any $t \geqslant 0$.

Case (ii) Assume that $r_m e^{-d_j\tau} > d_m$. With L defined as above and $l = \min_{\theta\in[-\tau,\,0]}\{\phi_s(\theta) + \phi_i(\theta)\}$, it follows that $h = \frac{1}{2}\min\{l, N_M^*\}$ and $H = 1 + \max\{L, N_M^*\}$ with $L > l > 0$. We claim that $h < N_M(t) < H$ for any $t \geqslant 0$. Otherwise there exists a $\bar{t} > 0$ such that $N_M(\bar{t}) = H$ and $N_M(t) < H$ for any $t < \bar{t}$. From (2.3),

$$\frac{dN_M(\bar{t})}{dt} = r_m N_M(\bar{t} - \tau)e^{-d_j\tau}e^{-\alpha H} - d_m H < H(r_m e^{-d_j\tau}e^{-\alpha H} - d_m) \leqslant 0.$$

The last inequality is true since $H > N_M^*$. But the definition of $\bar{t}$ implies $\frac{dN_M(\bar{t})}{dt} \geqslant 0$, a contradiction. Hence $N_M(t) < H$ for any $t \geqslant 0$. Similarly, we assume there exists a $\tilde{t} > 0$ such that $N_M(\tilde{t}) = h$, $N_M(t) > h$ for any $t < \tilde{t}$, and $\frac{dN_M(\tilde{t})}{dt} \leqslant 0$. Again from (2.3), since $h \leqslant N_M^*$,

$$\frac{dN_M(\tilde{t})}{dt} = r_m N_M(\tilde{t} - \tau)e^{-d_j\tau}e^{-\alpha h} - d_m h > h(r_m e^{-d_j\tau}e^{-\alpha h} - d_m) \geqslant 0,$$

a contradiction. Therefore, $h < N_M(t) < H$ for any $t \geqslant 0$.

In order to prove the global stability of N_M^*, we denote the right hand side of (2.3) as $f(N_M(t), N_M(t-\tau))$. Since $\frac{\partial f(x,y)}{\partial y} > 0$, it follows that (2.3) generates an eventually strongly monotone semiflow on the space C of continuous function on $[-\tau,0]$ with the usual pointwise ordering (see Smith [32]). If $r_m e^{-d_j\tau} \leqslant d_m$, there exists only a single trivial equilibrium $N_M = 0$. By Theorem 2.3.1 in [32], the equilibrium $N_M = 0$ is globally asymptotically stable. If $r_m e^{-d_j\tau} > d_m$, there are two equilibria $N_M = 0$ and N_M^*. By Theorem 2.3.2 in [32], solutions of (2.3) converges to one of the equilibria. To eliminate the possibility of $N_M = 0$ as the attractor, we linearize the system about $N_M = 0$ and use Theorem A2 in [10] to conclude that it is unstable when $r_m e^{-d_j\tau} > d_m$. Hence $N_M(t) \to N_M^*$ as $t \to \infty$. $\square$

Note that, using a similar argument to that in the proof of Theorem 2.1, we can show that if the total number of mosquitoes is initially less than N_M^*, then $N_M(t) < N_M^*$ for any finite $t \geqslant 0$; whereas if the total number of mosquitoes is initially greater than N_M^*, then $N_M(t) > N_M^*$ for any finite $t \geqslant 0$.

3. Classification of equilibria and dynamics of the full model

We now study the full mosquito and bird system.

Theorem 3.1. *Solutions of (2.1) with initial data (2.2) are positive and bounded for any finite time $t \geqslant 0$ and*

$$\lim_{t\to\infty} B_i(t) = 0, \quad \int_0^\infty B_i(t)dt < \infty.$$

In addition, there are the following two cases.

(i) *If $r_m e^{-d_j\tau} \leqslant d_m$, then $\lim_{t\to\infty}M_s(t) = 0$ and $\lim_{t\to\infty}M_i(t) = 0$.*
(ii) *If $r_m e^{-d_j\tau} > d_m$, then $\lim_{t\to\infty}M_s(t) = N_M^*$ and $\lim_{t\to\infty}M_i(t) = 0$.*

Proof. First we show that $M_s(t) > 0$ and $M_i(t) > 0$ for any finite $t \geqslant 0$. Otherwise assume that the susceptible mosquitoes reach zero first. Noting that $M_s(t) > 0$ for $t \in [-\tau,0]$, then there exists a $t' > 0$, such that $M_s(t') = 0$. Let $t_0 = \inf\{t > 0 | M_s(t) = 0\}$. It follows that $M_s(t) > 0$ and $M_i(t) > 0$ for $t \in [-\tau, t')$. From system (2.1),

$$\frac{dM_s(t_0)}{dt} = \begin{cases} r_m e^{-d_j\tau}e^{-\alpha(M_s(t_0)+M_i(t_0))}(\phi_s(t_0 - \tau) + (1-q)\phi_i(t_0 - \tau)), \\ \quad 0 \leqslant t_0 \leqslant \tau, \\ r_m e^{-d_j\tau}e^{-\alpha(M_s(t_0)+M_i(t_0))}(M_s(t_0 - \tau) + (1-q)M_i(t_0 - \tau)), \\ \quad t_0 > \tau. \end{cases}$$

Then $\frac{dM_s(t_0)}{dt} > 0$. But the definition of t_0 implies $\frac{dM_s(t_0)}{dt} \leqslant 0$, giving a contradiction. Thus $M_s(t) > 0$ for finite $t \geqslant 0$. Similarly it can be proved that $M_i(t) > 0$ for finite $t \geqslant 0$. The boundedness of $M_s(t)$ and $M_i(t)$ follows from Theorem 2.1.

Next we consider each class of birds. From (2.1),

$$B_s(t) = B_s(0)\exp\left(-\int_0^t \frac{\beta_b M_i(s)}{N_B(s)}ds\right) > 0 \quad \text{for } t \geqslant 0.$$

To prove that $B_i(t) > 0$ and $B_r(t) > 0$, we use the method of contradiction. Since $B_r(t)$ increases whenever $B_i(t)$ is positive, without loss of generality, we assume that $B_i(t)$ reaches zero first at some $\hat{t} > 0$. For $t < \hat{t}$, $B_i(t) > 0$ and $B_r(t) > 0$. From (2.1),

$$\frac{dB_i(\hat{t})}{dt} = \frac{\beta_b M_i(\hat{t})B_s(\hat{t})}{N_B(\hat{t})} > 0,$$

since $N_B(\hat{t}) = B_s(\hat{t}) + B_i(\hat{t}) + B_r(\hat{t}) = B_s(\hat{t}) + B_r(\hat{t}) > 0$. This gives a contradiction. Hence $B_i(t) > 0$ for any finite $t > 0$. It follows that $B_r(t) > 0$. The total bird population $N_B(t) = B_s(t) + B_i(t) + B_r(t) > 0$ is decreasing due to the disease induced death in the infectious birds, with a lower limit of zero. Hence each class of birds is bounded.

Using the method in [3], we first prove that $\lim_{t\to\infty}B_i(t) = 0$. Addition of the equations of (2.1) for susceptible and infectious birds gives

$$\frac{d(B_s + B_i)}{dt} = -(\mu + v)B_i.$$

Integration with respect to t from 0 to ∞ gives

$$B_s(0) + B_i(0) - B_{s,\infty} - B_{i,\infty} = (\mu + v)\int_0^\infty B_i(t)dt,$$

where $B_{s,\infty} = \lim_{t\to\infty}B_s(t)$ and $B_{i,\infty} = \lim_{t\to\infty}B_i(t)$. The left side is finite since $B_s(0)$, $B_i(0)$, $B_{s,\infty}$, and $B_{i,\infty}$ are bounded by the initial total population size. Therefore, $\int_0^\infty B_i(t)dt < \infty$. Since $B_i(t)$ is smooth and non-negative, it follows that $B_{i,\infty} = 0$ and

$$\int_0^\infty B_i(t)dt = \frac{1}{\mu + v}(B_s(0) + B_i(0) - B_{s,\infty}).$$

Case (i) Assume $r_m e^{-d_j\tau} \leqslant d_m$. By Theorem 2.1.i), it follows that $N_M(t) \to 0$. Hence $M_s(t) + M_i(t) \to 0$. Since $M_s(t)$ and $M_i(t)$ are non-negative, $M_s(t) \to 0$ and $M_i(t) \to 0$ as $t \to +\infty$.

Case (ii) Assuming $r_m e^{-d_j\tau} > d_m$, Theorem 2.1.ii) gives $\lim_{t\to\infty}N_M(t) = N_M^*$. Since $\lim_{t\to\infty}B_i(t) = 0$, the equation for infectious mosquitoes is asymptotically autonomous with limit equation

$$\frac{dy}{dt} = qr_m y(t - \tau)e^{-d_j\tau}e^{-\alpha N_M^*(t)} - d_m y. \tag{3.1}$$

Eq. (3.1) has only a trivial equilibrium $y = 0$ and it is globally asymptotically stable (see [22, p. 32]). By Corollary 4.3 in [33], $\lim_{t\to\infty}M_i(t) = 0$, and thus $\lim_{t\to\infty}M_s(t) = N_M^*$. $\square$

The equilibria of system (2.1) are obtained by setting the right hand side to zero. In the presence of West Nile virus, $B_s(t)$ is strictly decreasing and therefore the model exhibits no endemic equilibrium. On the other hand, system (2.1) always has an infinite number of equilibria. More precisely, we observe the following.

(i) The first type of disease-free equilibrium with no mosquitoes $E_{01} = (0, 0, \bar{B}_s, 0, \bar{B}_r)$ always exists with arbitrary $\bar{B}_s$ and $\bar{B}_r$.

(ii) If $r_m e^{-d_j\tau} > d_m$, system (2.1) has an infinite number of the second type of disease-free equilibria with mosquitoes and birds given by $E_{02} = (N_M^*, 0, \widetilde{B}_s, 0, \widetilde{B}_r)$ with arbitrary $\widetilde{B}_s$ and $\widetilde{B}_r$.

Linearizing the system (2.1) about E_{01}, we obtain the characteristic equation as

$$z^2(\mu + \nu + z)(-d_m - z + r_m e^{-(d_j+z)\tau})(-d_m - z + q r_m e^{-(d_j+z)\tau}) = 0. \tag{3.2}$$

Eq. (3.2) has three roots 0, 0 and $-(\mu + \nu)$, with all other eigenvalues determined by roots of

$$(d_m + z - r_m e^{-(d_j+z)\tau})(d_m + z - q r_m e^{-(d_j+z)\tau}) = 0.$$

Linearizing at the equilibrium $E_{02} = (N_M, 0, \widetilde{B}_s, 0, \widetilde{B}_r)$ yields the characteristic equation

$$z^2(z - d_m e^{-z\tau} + d_m(1 + \alpha N_M^*))(z^2 + (\mu + \nu + d_m)z + (d_m(\mu + \nu)$$
$$- \frac{\beta_b \widetilde{B}_s \beta_m N_M^*}{(N_B^*)^2}) - e^{-z\tau} q d_m(z + \mu + \nu)) = 0. \tag{3.3}$$

However, due to the existence of a continuous curve of equilibria, 0 is a double zero eigenvalue together of both characteristic equations (3.2) and (3.3). This existence of a double zero eigenvalue together with the fact that initial values also appear in the coefficients of the characteristic Eq. (3.3) shows that both types of equilibria are in a critical case and E_{02} is a degenerate singularity. The study of such a degeneracy from a bifurcation point of view is out of the scope of this study. Indeed, we will see in our simulations (Section 4), this degeneracy may give rise to some transient multiple peaks of infection. Despite this difficulty, we do have a full picture of the global asymptotic dynamics as now described.

Theorem 3.2. *If $r_m e^{-d_j\tau} \leqslant d_m$, then $(M_s(t), M_i(t), B_s(t), B_i(t), B_r(t)) \to E_{01}$ as $t \to +\infty$, thus all mosquitoes and WNv infectious birds die out.*

Proof. By Theorem 3.1.i), $M_s(t) \to 0$ and $M_i(t) \to 0$; i.e. the mosquitoes eventually die out. From results of [9], the limit equations for the bird population are $\frac{dB_s}{dt} = 0$, $\frac{dB_i}{dt} = -(\mu + \nu)B_i$, and $\frac{dB_r}{dt} = \nu B_i$. Hence $(B_s(t), B_i(t), B_r(t)) \to (\overline{B}_s, 0, \overline{B}_r)$ as $t \to \infty$. □

Theorem 3.3. *If $r_m e^{-d_j\tau} > d_m$, then for any solution of (2.1) with initial data (2.2), there exists $\widehat{B}_s \geqslant 0$ and $\widehat{B}_r \geqslant 0$ such that*

$$(M_s(t), M_i(t), B_s(t), B_i(t), B_r(t)) \to (N_M^*, 0, \widehat{B}_s, 0, \widehat{B}_r), \quad \text{as } t \to \infty.$$

Proof. We first show that if $r_m e^{-d_j\tau} > d_m$, then E_{02} is unstable. For any $\epsilon > 0$, consider a solution with constant initial data $(N_M^* - \epsilon, \epsilon, \widetilde{B}_s - \epsilon, 0, \widetilde{B}_r + \epsilon)$ close to E_{02}. By Theorem 3.1.ii), $M_s(t) \to N_M^*$, $M_i(t) \to 0$, and $B_i(t) \to 0$ as $t \to \infty$. Since $B_s(t)$ is decreasing with lower bound 0, there exists $0 \leqslant \widehat{B}_s < \widetilde{B}_s$ such that $B_s(t) \to \widehat{B}_s$ as $t \to \infty$. Noting that $B_r(t)$ increases with an upper bound of the total initial bird population, there exists $\widehat{B}_r > \widetilde{B}_r$ such that $B_r(t) \to \widehat{B}_r$ as $t \to \infty$. □

4. Numerical simulations

Throughout this section, for all simulations, we use constant initial data on the interval $[-\tau, 0]$, and take parameters so that $r_m e^{-d_j\tau} > d_m$. For Figs. 1–3, all parameters are as collected and given in Table 1. For such choice of parameters, $N_M^* \approx 28361$. Any point $E_{02} = (N_M^*, 0, \widetilde{B}_s, 0, \widetilde{B}_r)$ with $(\widetilde{B}_s, \widetilde{B}_r)$ in the non-negative quadrant of the B_sB_r- plane is a second type of disease-free equilibrium. For the mosquito population, we use initial data $(M_s(t), M_i(t))$ $=(28000, 100)$ for $t \in [-\tau, 0]$ so that mosquitoes are close to their
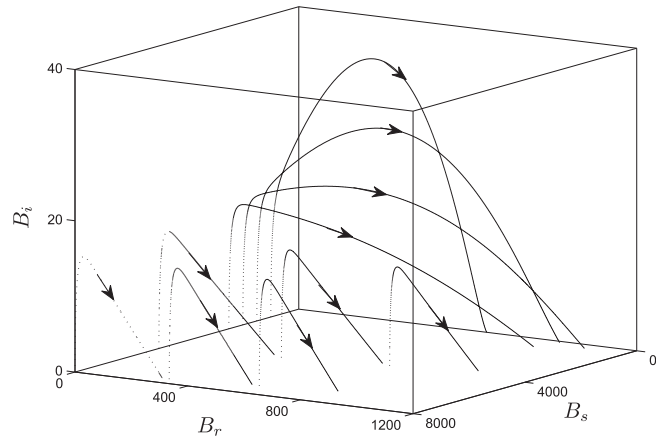

Fig. 1. Simulations using parameters from Table 1. The phase portrait in (B_s, B_r, B_i) coordinates with $B_i(0) = 0$, $B_s(0)$ varying from 1000 to 8000 and $B_r(0)$ varying from 0 to 800. Each orbit approaches a different equilibrium E_{02} depending on the initial data.
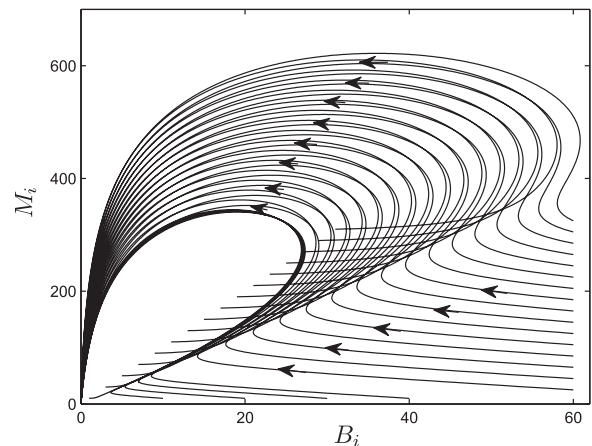

Fig. 2. The phase portrait in the (B_i, M_i)-plane for parameters as given in Table 1. For different orbits, there are different initial data with $M_i(t) = M_{i0}$ for $t \in [-\tau, 0]$ and $B_i(0) = B_{i0}$ where $M_{i0} \in [50, 2000]$ and $B_{i0} \in [10, 900]$. All orbits approach $(0,0)$ along the vertical axis as $t \to \infty$.

steady state $(N_M^*, 0)$. For the bird population, we choose initial values in the B_sB_r- plane. Simulations using parameters from Table 1 are given in Fig. 1. From this figure, it can be seen that each orbit leaves its starting point and approaches another equilibrium in the B_sB_r- plane which has smaller B_s and larger B_r values. None of the equilibrium E_{02} in the B_sB_r- plane is stable except $\widetilde{B}_s = 0$.

In order to illustrate the transient and asymptotic behaviors of infectious classes (mosquitoes and birds), we fix initial data for susceptible and recovered classes ($M_s(t) = 28000$ for $t \in [-\tau, 0]$ for mosquitoes, $B_s(0) = 1000$ and $B_r(0) = 0$ for birds). Varying the initial data of the infectious classes, Fig. 2 shows that even if there are only a small number of mosquitoes or birds or both that are infectious at the beginning, the infectious classes have a chance to increase before they eventually return to zero again as predicted in Theorem 3.1. From Fig. 2, we notice that usually the number of infectious birds reaches its peak before the number of infectious mosquitoes reaches its peak. This remains true even when maturation delay varies (see Fig. 3). Depending on the initial data, we also notice that (simulations not presented here) an alternative case can also happen with the infectious mosquitoes first reaching their peak but the infectious birds monotonically decreasing to zero.
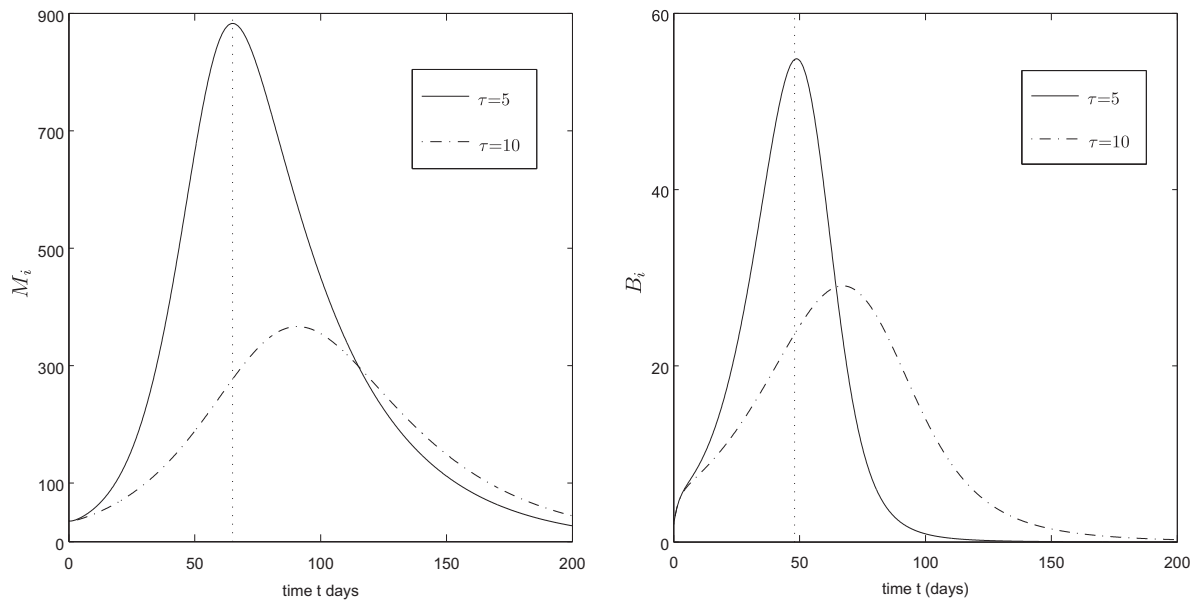
Fig. 3. The time evolution of infectious mosquitoes (LEFT) and birds (RIGHT) for values $\tau = 5$ and 10 days. All parameters are as given in Table 1. Initial data $(M_s(t), M_i(t)) = (28\,000, 35)$ for $t \in [-\tau, 0]$ and $B_s(0) = 1000$, $B_i(0) = 2$ and $B_r(0) = 0$. The vertical dotted line indicates the time of peaks $t \approx 48$ days for birds and $t \approx 65$ days for mosquitoes.

Table 1
Parameters for Figs. 1–3. Time unit is one day and rates are daily.

| Parameter	Description	Mean (Range)	Resource
r_m	Average number of eggs laid per female mosquito	20 (0.036–42.5)	[38]
β_m	Effective contact transmission rate from birds to mosquitoes	0.0144 (0.0006–0.384)	[38]
β_b	Effective contact transmission rate from mosquitoes to birds	0.08 (0.024–0.16)	[38]
d_m	Mosquito adult per capita mortality rate	0.029 (0.016–0.07)	[38]
μ	WNv induced per capita mortality rate of birds	0.143 (0.125–0.2)	[38]
v	Recovery rate of infectious birds	0.3 (0.18–0.36)	[21]
τ	Maturation delay of mosquitoes	10 (5–30)	[26,17]
d_j	Death rate of immature mosquitoes	0.37 (0.28–0.46)	[29,35]
$1/\alpha$	Size of mosquito population at which egg laying is maximized without delay	10000	[16,17]
q	Vertical transmission rate in mosquitoes	0.007	[13,15]

In order to better visualize the impact of maturation delay τ and vertical transmission rate q, we carry out numerical simulations of system (2.1) by varying τ and q in the case of a WNv epidemic for a different set of parameters as used in [12], see the caption of Fig. 4. The initial conditions are taken to be: $M_s(\theta) = 90\,000$, $M_i(\theta) = 5000$ for $\theta \in [-\tau, 0]$, $B_s(0) = 50\,000$, $B_i(0) = 100$, and $B_r(0) = 50$. In Fig. 4, when τ increases from 5 to 10, then to 15 days, the number of susceptible mosquito increases initially and then stabilizes at a positive level ($N_M^* \approx 9.35 \times 10^8$, 8.35×10^8, or 7.35×10^8 respectively), which decreases with τ. The smaller the delay, the quicker the population reaches its stable level. The number of infectious mosquitoes has two peaks, and decreases monotonically after its second peak for each delay value, and the infectious mosquitoes attain their first peak almost at the same time (≈ 9 days). But the amplitudes of the peaks are different. The smaller the delay, the larger the peak. For a second peak, both the amplitude and the peaking time vary with delay. For $\tau = 10$ days, the second peak is even higher than the first peak. But for $\tau = 20$ and 30 days, the second peak is lower than the first. For each curve, the time between

the two peaks is approximately equal to the time delay used for the simulation. The susceptible birds decrease monotonically, and decrease slower as τ increases. The number of infectious birds increases first, reaches the peak within a short period of time, 3 days for $\tau = 10$, 3.5 days for $\tau = 20$, and 4.5 days for $\tau = 30$, and then decreases to zero quickly. As the delay increases, the peaking time increases and the amplitude of the peak decreases. In all cases, the infectious birds reach their peaks approximately 5 days earlier than the infectious mosquitoes.

To investigate the effects of vertical transmission of mosquitoes on the dynamical behaviors of the model, we take different q values with all other parameters fixed as in Fig. 4. We choose $q = 0.03$ and vary τ from 10 to 20, and then to 30 days. The numerical results demonstrate that the susceptible mosquitoes and birds behave similarly as with $q = 0.007$ for the corresponding delay values. But the behaviors of infectious mosquitoes and birds are different (see Fig. 5). In Fig. 5(a), for each delay, the infectious mosquitoes reach their first peak one day earlier than with $q = 0.007$, but the amplitude of the peak is almost the same. However the amplitude of the second peak
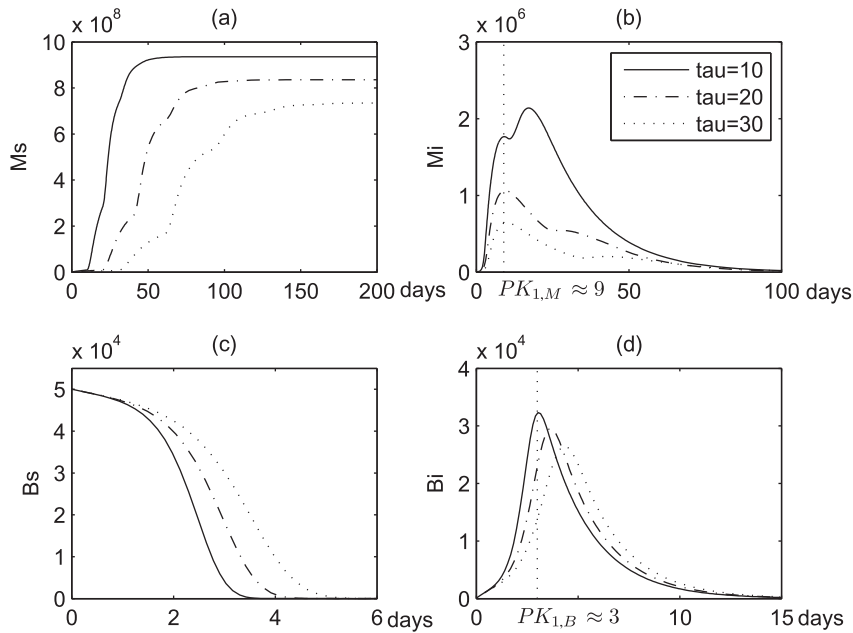
Fig. 4. The variation of mosquito and bird populations for three delay values τ = 10, 20, and 30 days. In each of the figures, the solid curve, the dash-dotted, and the dotted correspond to τ = 10, 20 and 30 days. In (b), the quantity $PK_{1,M}$ denotes the time at which the first peak of infectious mosquitoes is reached. For different delay values, the infectious mosquitoes reach their first peak almost at the same time 9 days. But the times for the second peak are different. For each curve, the time between those two peaks is approximately equal to the time delay. The second peak for τ = 10 is even higher than the first peak. But for τ = 20 and 30 days, the second peak is lower than the first peak. In (d), the quantity $PK_{1,B}$ denotes the time at which the first peak for infectious birds is reached. For τ = 10, 20, and 30 days, $PK_{1,B} \approx$ 3, 3.5 and 4.5 days. Parameters d_m = 0.06, β_m = 0.2, β_b = 0.5, μ = 0.08, q = 0.007, and v = 0.36 are taken from [12]. Other parameters r_m = 30, d_j = 0.06, α = 0.000000006 are estimated.
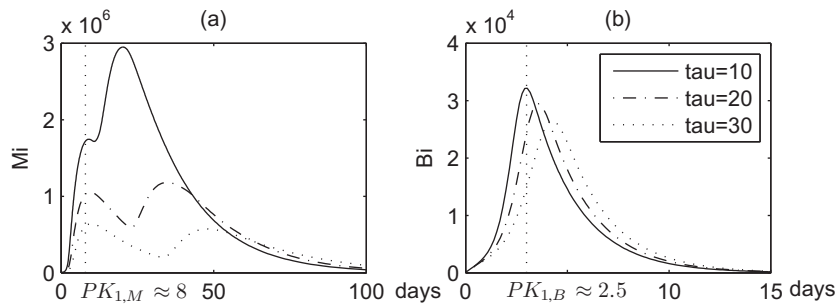
Fig. 5. The population dynamics of infectious mosquitoes and birds for three delay values τ = 10, 20, and 30 days. Parameter q = 0.03 and all other parameters are as in Fig. 4.

increases, getting close to or above the first peak. Also at the end of 100 days, a larger number of infectious mosquitoes remains alive. In Fig. 5(b), for each delay, the infectious birds reach their peak half a day earlier than with q = 0.007 and the amplitude is almost the

same. In Fig. 6(a) with q = 0.3, for τ = 20 and 30 days, the infectious mosquitoes have a third peak with amplitude greater than those of the first two peaks. Also the amplitude of the second peak is greater than that of the first peak. At the end of 100 days, there are still a lot of
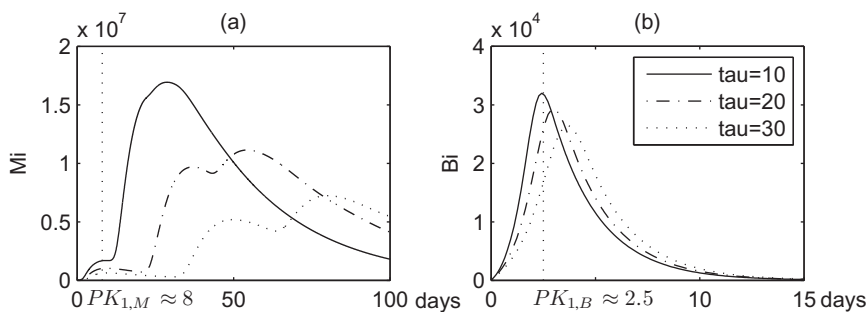
Fig. 6. The population of infectious mosquitoes and birds. Parameter q = 0.3 and all other parameters are as in Fig. 4.

infectious mosquitoes left, a number even larger than the infectious mosquitoes at the peaks when $q = 0.007$.

5. Discussion

In this paper, we consider a single-season model with time delay and vertical transmission. Here, the time delay is the maturation time of the mosquitoes, which reflects the effects of the temperature variation on the development of the aquatic stages of the mosquito. Our numerical results indicate that infectious birds reach their peak first (within 3–5 days) and then the infectious mosquitoes reach their first peak (about 8–10 days). This seems to suggest that the infectious birds drive the infectious mosquitoes to a peak. For infected mosquitoes, the time between two peaks is approximately equal to the maturation time. The increase of the vertical transmission rate has no big impact on the amplitude of the first peak. However if the vertical transmission rate becomes higher, there are multiple peaks appearing and the amplitudes of the second or later peaks can be even larger than the amplitude of the first peak. Vertical transmission increases the survival of West Nile virus in nature. Thus increased vertical transmission from adult mosquitoes to offspring increases the number of infectious mosquitoes and the risk of humans and other vertebrate animals being infected by WNv.

As pointed out in [7,18,27], within the limits of a lower development threshold and an upper lethal temperature, the aquatic stages of mosquitoes develop faster as temperature increases. Our numerical results indicate that more mosquitoes can be infected within a certain time period. Hence when temperature increases, the maturation time from egg to adult mosquito becomes shorter, and more mosquitoes can be infected. Thus increasing the temperature provides a better chance for the transmission of West Nile virus, and potentially increases the risk of human infection.

In North America, many areas carry out an annual mosquito control program. One of the commonly used methods is insecticide spraying to kill the flying adult mosquitoes. However, due to the vertical transmission of the virus, the mosquito eggs that carry the virus mature to carry on the transmission cycle of the virus in birds and mosquitoes and further cause human infection. In particular, increasing temperature in an area can speed up the hatching process of mosquito eggs even though insecticide spraying is applied. Therefore the combination of the impact of increasing temperature and the vertical transmission of the virus in the mosquitoes can cause an outbreak of the virus in an area even though an adult mosquito control program is applied. The dynamics of the interaction of increasing temperature and vertical transmission could explain the continuing activity of the virus in Southern Ontario and other places in Canada [40].

There are a number of other factors we have not considered in this paper. The diversity of bird species and their dispersion, migration, as well as latitudinal variation in host and vector population, all remain to be explored.

Acknowledgments

References

[1] J.F. Anderson, A.J. Main, Importance of vertical and horizontal transmission of West Nile virus by *Culex pipiens* in the Northeastern United States, J. Infect. Dis. 194 (11) (2006) 1577.
[2] R.M. Anderson, R.M. May, Infectious Diseases of Humans, Oxford University, London/New York, 1991.
[3] J. Arino, F. Brauer, P. vanden Driessche, J. Watmough, J. Wu, A final size relation for epidemic models, Math. Biosci. Eng. 4 (2) (2007) 159.
[4] J. Arino, L. Wang, G.S.K. Wolkowicz, An alternative formulation for a delayed logistic equation, J. Theor. Biol. 241 (1) (2006) 109.
[5] M.N. Bayoh, S.W. Lindsay, Effect of temperature on the development of the aquatic stages of *Anopheles gambiae sensu stricto* (*Diptera: Culicidae*), B. Entomol. Res. 93 (5) (2003) 375.
[6] C. Bowman, A.B. Gumel, P. van den Driessche, J. Wu, H. Zhu, A mathematical model for assessing control strategies against West Nile virus, B. Math. Biol. 67 (5) (2005) 1107.
[7] R. Brust, Weight and develpoment time of different stadia of mosquitoes reared at various constant temperature, Can. Entomol. 99 (9) (1967) 986.
[8] L.G. Campbell, A.A. Martin, R.S. Lanciotti, D.J. Guble, West Nile virus, Lancet Infect. Dis. 2 (9) (2002) 519.
[9] C. Castillo-Chavez, H.R. Thieme, Asympotically autonomous epidemic models, in: O. Arino (Ed.), Math. Population Dyn. Anal. Heterogeneity I. Theor. Epidemics, Wuerz, Canada, 1995, p. 33.
[10] K.L. Cooke, P. van den Driessche, Analysis of an SEIRS epidemic model with two delays, J. Math. Biol. 35 (2) (1996) 240.
[11] K.L. Cooke, P. van den Driessche, X. Zou, Interaction of maturation delay and nonlinear birth in population and epidemic models, J. Math. Biol. 39 (1999) 332.
[12] G. Cruz-Pacheco, L. Esteva, J.A. Montano-Hirose, C. Vargas, Modelling the dynamics of West Nile virus, B. Math. Biol. 67 (6) (2005) 1157.
[13] D.J. Dohm, M.R. Sardelis, M.J. Turell, Experimental vertical transmission of West Nile virus by *Culex pipiens* (*Diptera: Culicidae*), J. Med. Entomol. 39 (4) (2002) 640.
[14] C. Garett-Jones, Prognosis for interruption of malaria transmission through assessment of mosquitoes vectorical capacity, Nature 204 (1964) 1173.
[15] L.B. Goddard, A.E. Roth, W.K. Reisen, T.W. Scott, Vertical transmission of West Nile virus by three California Culex (*Diptera: Culicidae*) species, J. Med. Entomol. 40 (6) (2003) 743.
[16] S.A. Gourley, R. Liu, J. Wu, Eradicating vector-borne disease via age-structured culling, J. Math. Biol. 54 (3) (2007) 309.
[17] S.A. Gourley, R. Liu, J. Wu, Some vector borne disease with structured host populations: extinction and spatial spread, SIAM J. Appl. Math. 67 (2) (2007) 408.
[18] D.W. Hagstrum, E.B. Workman, Interaction of temperature and feeding rate in determining the rate of development of larval *Culex tarsalis*, Ann. Entomol. Soc. Am. 64 (3) (1971) 668.
[19] H. Hethcote, The mathematics of infectious diseases, SIAM Rev. 42 (4) (2000) 599.
[20] C. Huffaker, The temperature relations of the immature stages of the malarial mosquito *An. quadrimaculatus Say*, with a comparison of the developmental power of constant and variable temperatures in insect metabolism, Ann. Emtomol. Soc. Am. 37 (1) (1944) 1.
[21] N. Komar, S. Langevin, N. Nemeth, E. Edwards, D. Hettler, B. Davis, R. Bowen, M. Bunning, Experimental infection of North American birds with the New York 1999 strain of West Nile virus, Emerg. Infect. Dis. 9 (3) (2003) 11.
[22] Y. Kuang, Delay differential equation with applications in population dynamics, Academic Press, Boston, 1993.
[23] S.A. Langevin, M. Bunning, N.K.B. Davis, Experimental infection of chickens as candidate sentinels for West Nile virus, Emerg. Infect. Dis. 7 (4) (2001) 726.
[24] M. Lassiter, C. Apperson, R. Roe, Juvenile hormone metabolism during the fourth stadium and pupal stage of the south house mosquito *Culex quinquefasciatus Say*, J. Insect Physiol. 41 (10) (1995) 869.
[25] M. Lewis, J. Renclawowicz, P. van den Driessche, Travelling waves and spread rates for a West Nile virus model, B. Math. Biol. 68 (1) (2006) 3.
[26] C.C. Lord, J.F. Day, Simulation studies of St. Louis encephalitis and West Nile viruses: the impact of bird mortality, Vector Borne Zoonotic Dis. 1 (4) (2001) 317.
[27] E.O. Lyimo, W. Takken, Effects of adult body size on fecundity and the pre-gravid rate of *Anopheles gambiae* females in Tanzania, Med. Vet. Entomol. 7 (4) (1993) 328.
[28] R.G. Mclean, S.R. Ubico, D.E. Docherty, W.R. Hansen, L. Sileo, T.S. McNamara, West Nile virus transmission and ecology in birds, Ann. NY Acad. Sci. 951 (2001) 54.
[29] S. Munga, N. Minakawa, G. Zhou, Survivorship of immature stages of *Anopheles gambiae* s.l. (*Diptera: Culicidae*) in natural habitats in western Kenya highlands, J. Med. Entomol. 44 (5) (2007) 758.
[30] K.P. Paaijmans, A.F. Read, M.B. Thomas, Understanding the link between malaria risk and climate, Proc. Natl. Acad. Sci. USA 106 (33) (2009) 13844.
[31] J. Shaman, M. Spiegelman, M. Cane, M. Stieglitz, A hydrologically driven model of swamp water mosquito population dynamics, Ecol. Model. 194 (2006) 395.
[32] H.J. Smith, Monotone dynamical systems: an introduction to the theory of competitive and cooperative systems, Mathematical Surveys and Monographs, vol. 41, American Mathematical Society, Providence Rhode Island, 1995.
[33] H.R. Thieme, Convergence results and a Poincaré-Bendixson trichotomy for asymptotically autonomous differential equations, J. Math. Biol. 30 (7) (1992) 755.
[34] W. Tun-Lin, T.R. Burkot, B.H. Kay, Effect of temperature and larval diet on development rate and survival of the dengue vector *Aedes aegypti* in north Queensland, Australia, Med. Vet. Entomol. 14 (1) (2000) 31.

[35] N. Tuno, W. Okeka, N. Minakawa, M. Takagi, Survivorship of *Anopheles gambiae* sensu stricto (*Diptera: Culicidae*) larvae in western Kenya highland forest, J. Med. Entomol. 42 (3) (2005) 270.

[36] J.X. Velasco-Hernández, A model for Chagas disease involving transmission by vectors and blood transfusion, Theor. Popul. Biol. 46 (1) (1994) 1.

[37] H. Wan, H. Zhu, The backward bifurcation in compartmental models for West Nile virus, Math. Biosci. 227 (2010) 20.

[38] M.J. Wonham, T. de-Camino Beck, M.A. Lewis, An epidemiological model for West Nile virus: invasion analysis and control applications, Proc. Roy. Soc. Lond. Ser. B 271 (1538) (2004) 501.

[39] <http://www.cdc.gov/ncidod/dvbid/westnile/>.

[40] <http://www.phac-aspc.gc.ca/wnv-vwn/index-eng.php>.